Staircase modulation wave form for continuum source atomic absorption spectrometry

ARTICLE *in* ANALYTICAL CHEMISTRY · FEBRUARY 1984

Impact Factor: 5.64 · DOI: 10.1021/ac00266a013

3 AUTHORS:

Nancy Miller-Ihli
Savvy Selections
47 PUBLICATIONS **1,393** CITATIONS
SEE PROFILE

Tom Calvin O'Haver
University of Maryland, College Park
81 PUBLICATIONS **1,446** CITATIONS
SEE PROFILE

James Harnly
Agricultural Research Service
163 PUBLICATIONS **3,397** CITATIONS
SEE PROFILE

Staircase Modulation Wave Form for Continuum Source Atomic Absorption Spectrometry

N. J. Miller-Ihli[1] and T. C. O'Haver*

Department of Chemistry, University of Maryland, College Park, Maryland 20742

J. M. Harnly

Nutrient Composition Laboratory, U.S. Department of Agriculture, Beltsville, Maryland 20705

A new staircase modulation wave form is implemented for extended range continuum source AAS measurements, which improves performance and simplifies the computation of concentrations. This wave form facilitates the computation of two absorbances of different sensitivity for every atomization. The resulting two calibration curves allow 4–6 orders of magnitude of concentration to be covered effectively. Calibration curves and concentration error curves are compared for Mn, Zn, Fe, Cu, and Mg with the old bi-Gaussian and the new staircase modulation wave forms. Linearities, sensitivities, and SNR's of the curves obtained by using the two modulation wave forms are compared. In addition, accuracy using the staircase modulation wave form was evaluated by running National Bureau of Standards (NBS) standard reference materials (SRM's).

In previous papers (*1*, *2*) we have described a simultaneous multielement atomic absorption spectrometer (SIMAAC) based upon a continuum primary light source and a high-resolution, wavelength-modulated, direct-reading spectrometer. One of the problems which must be overcome in such a system is the limited concentration range which is ordinarily considered to be characteristic of atomic absorption measurement. In previous work (*1*) we have achieved a greatly extended working concentration range by measuring the absorbance at several wavelengths across the profile of a single analytical absorption line (Figure 1). The absorbance at the line center is utilized at low to medium concentrations. At higher concentrations, where the absorbance at the line center is too high to be useful, the system automatically utilizes the absorbances measured on the sides of the absorption profile. Because it is not practical to control the wavelength modulation interval individually for each element in response to its concentration in each sample, the system has been designed to acquire and store a fixed pattern of points across the entire absorption profile of each element. In our previous work sufficient data have been taken to allow the calculation of six double-beam, background-corrected absorbances of different sensitivities. Thus, when the system is calibrated (as usual by the measurement of a series of standard solutions), the six absorbances measured for each calibration solution are used to prepare a set of six analytical curves. When an unknown sample is measured, it too produces six absorbance readings, each of which is read off the corresponding analytical curves to give a set of six estimates of the sample concentration. Ideally, the six estimates of the concentration should be identical but, because of noise and curve-fitting errors, they will never be exactly the same. Moreover, they will not be equally useful; at low sample concentrations, the measurements taken far from the line center will be unusable because of poor signal-to-noise ratio (SNR), whereas at high sample concentrations, measurements taken near the line center will be unusable because of curve-fitting errors. The selection of the optimum concentration estimate, or the optimum combination of concentration estimates, can be done in a number of ways. We have based our selection on the observation of relative concentration errors (RCE), which are calculated in the following way. For each sample measured by flame atomization, the integration period (5 s) is divided into 28 equal segments over which each of the six absorbances is calculated. This yields an estimate of the mean and standard deviation of each of the six absorbances. Each of these is converted into an equivalent mean and standard deviation of concentration by utilizing the corresponding analytical curve in conjunction with some method of curve fitting or interpolation. The relative concentration error is the ratio of the standard deviation of concentration to the mean concentration. In our work we have computed the reported concentration for each sample solution based on the weighted average of the six concentration estimates, where the weighting factor is taken as the square of the SNR (1/RCE). Thus, each of the concentration estimates is utilized to the extent that it can contribute useful information.

The use of six analytical curves seems reasonable when one inspects plots of the analytical curves themselves; the linear ranges of the curves overlap over a total concentration range of 4–6 orders of magnitude. However, the manipulation of six absorbances and six analytical calibrations considerably complicates the computer software. Moreover, a critical inspection of plots of RCE vs. concentration shows that not all curves are really necessary. A typical case is that for copper at 324.7 nm, shown in Figure 2. It can be seen here that the regions of lowest RCE on each curve overlap extensively. This is due to the fact that, by utilizing appropriate curve-fitting procedures, the useful region of each analytical curve can be extended considerably above the upper limit of analytical curve linearity. As a result it is possible to achieve quite acceptably low values of RCE over 5 orders of magnitude of concentration by using only two curves, curves 1 and 4.

In our system the data acquisition rate during the wavelength modulation cycle is constant; therefore, the distribution of the measured points with respect to wavelength is determined by the shape of the modulation wave form. For line profile measurements we use a triangular wave form, which gives a uniform point distribution. On the other hand, for quantitative analytical applications, a bi-Gaussian wave form has been used. This wave form results in a concentration of points near the center of the line profile (Figure 1) which allows the most sensitive (curve 1) absorbance to be calculated from the average of 20 intensity readings, resulting in a reduction of random noise (including quantization noise). The less sensitive absorbances, however, are calculated from four

[1] Present address: U.S. Department of Agriculture, Building 161, BARC-East, Beltsville, MD 20705.

0003-2700/84/0356-0176$01.50/0

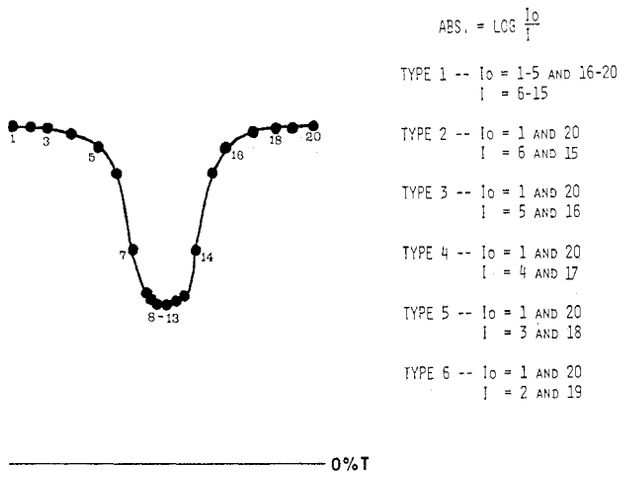

Figure 1. Absorption profile for 50 μg/mL sodium and the point combinations for the six types of absorbance computations (bi-Gaussian wave form).

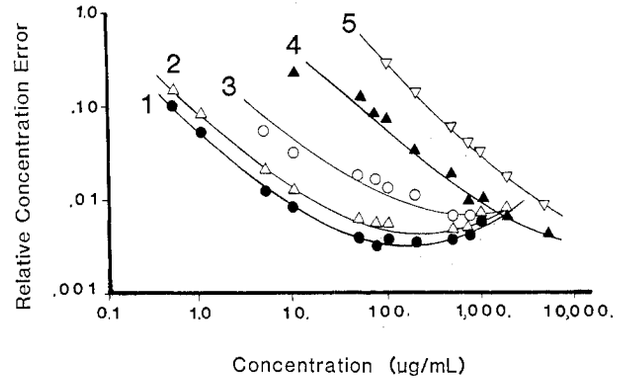

Figure 2. Relative concentration error curves for copper (324.754 nm) using the bi-Gaussian modulation wave form.

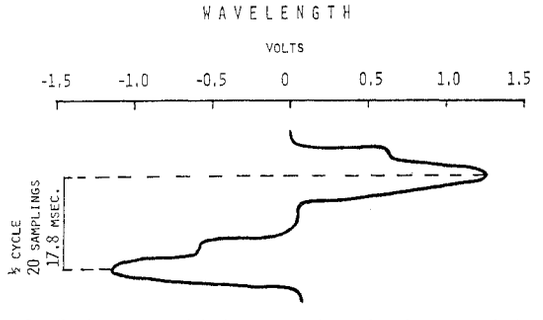

Figure 3. Staircase modulation wave form for the extended range.

intensity readings and therefore tend to be noiser. The theoretical difference in absorbance SNR's is 2.24 (equal to $(20/4)^{1/2}$). It is for this reason that the RCE for the less sensitive curves never achieves as low a value as that of the most sensitive curve (cf. Figure 2). As a result, the precision of measurement of high concentrations is slightly poorer than it might otherwise be.

In this paper we describe a modified staircase modulation wave form which both simplifies the calculations and improves the performance of quantitative analytical calibration on the SIMAAC system. The new wave form, shown in Figure 3, concentrates the measured points into five regions, as shown in Figure 4, which allows the computation of two double-beam, background-corrected absorbances. The most sensitive (primary) absorbance utilizes all 20 measured points and corresponds to curve 1 in the previous system, whereas the less sensitive (secondary) absorbance utilizes 12 points and corresponds closely to the old curve 4.

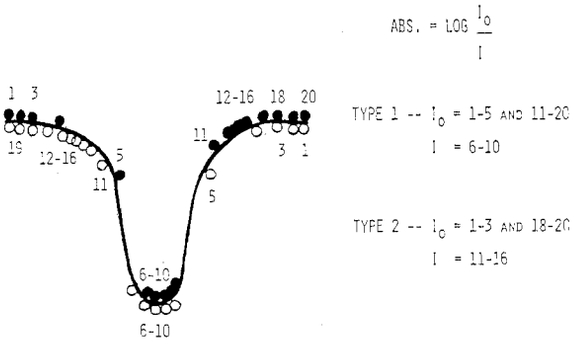

Figure 4. Absorption profile for 50 μg/mL sodium and the point combinations for the two types of absorbance computations (staircase wave form).

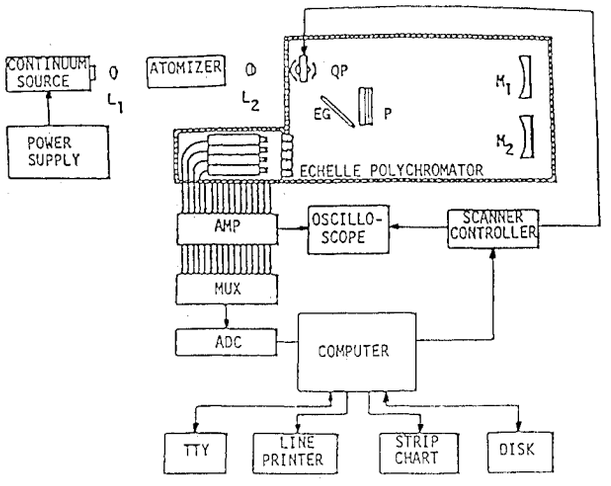

Figure 5. Block diagram of the SIMAAC system: L_1 and L_2, lenses; QP, quartz plate; EG, echelle grating; P, prism; M_1 and M_2, mirrors; AMP, amplifier, MUX, multiplexer; ADC, analog-to-digital converter; TTY, teletype scope.

EXPERIMENTAL SECTION

Instrumentation. The SIMAAC system has been described previously (*2, 3*) and the physical configuration is shown in Figure 5. Briefly, the system consists of an echelle polychromator modified for wavelength modulation, a continuum source, and a dedicated minicomputer. The only modification of the SIMAAC system was the installation of a 6-mm quartz refractor plate in place of the 3-mm plate. This was done so that the same modulation intervals (*1*) could be obtained with half of the angle of rotation of the quartz plate. The advantage of decreased movement of the quartz plate is that positional control and precision are improved.

Simultaneous multielement data were obtained by using flame atomization (*4*). A lean air–acetylene flame (air flow, 12.5 L/min; acetylene flow, 2.6 L/min) was employed for all measurements. All measurements were made 1.5 mm above the burner head.

All line source analyses were performed on a Perkin-Elmer 603, using optimum conditions for each element.

Calibration Standards. Multielement calibration standards were made by using multielement stock solutions from Spex Industries (Metuchen, NJ). Standards were diluted to a final HNO_3 acid concentration of 5% using Ultrex HNO_3 (J. T. Baker, Phillipsburg, NJ). Nine standards were used to cover 4 orders of magnitude of concentration (0.1 to 1000 μg/mL, Fe, Mg, Ca, Na, and K, and 0.01 to 100 μg/mL Mn, Zn, Cu, Cr, Ni, and Co).

Standard Reference Materials. Four National Bureau of Standards (NBS) standard reference materials (SRM's) were analyzed: wheat flour (1567), rice flour (1568), bovine liver (1577), and spinach (1570). The suggested amount of each reference material was weighed into a test tube. Samples were digested by using a wet ash (HNO_3/H_2O_2) method (*5*). Digests were brought to a volume of 10 mL and analyzed. Each SRM was prepared in triplicate. The SIMAAC system was used in the multielement mode with an air–acetylene flame for simultaneous

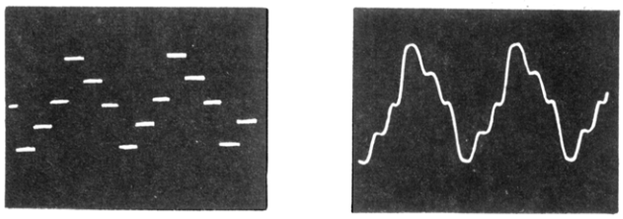

Figure 6. Digital-to-analog converter output and the torque motor response for the staircase modulation wave form.

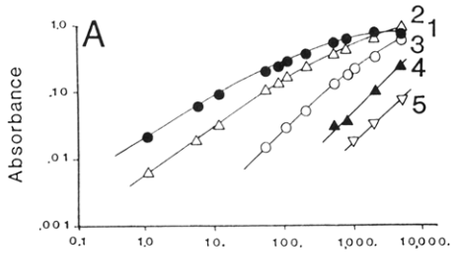

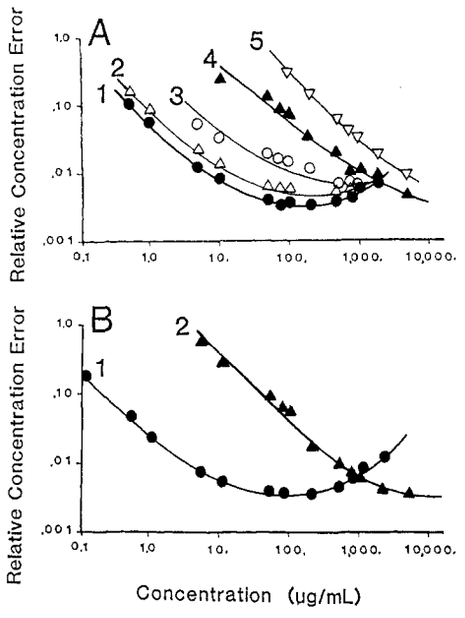

Figure 10. Relative concentration error curves for copper (324.754 nm) in an air–acetylene flame using: (A) bi-Gaussian and (B) staircase modulation wave form.

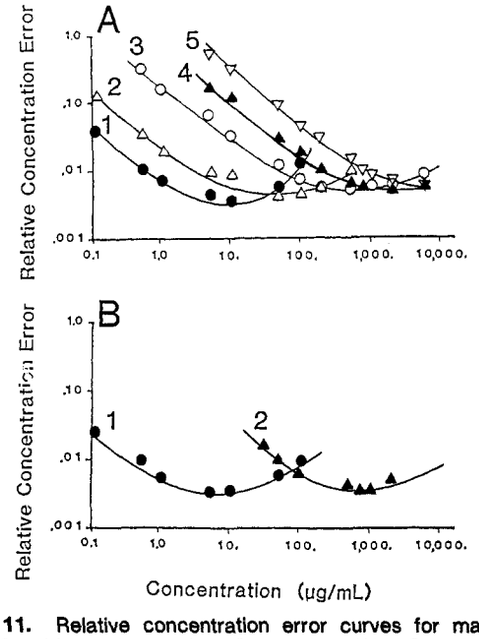

Figure 11. Relative concentration error curves for magnesium (285.213 nm) in an air–acetylene flame using: (A) bi-Gaussian and (B) staircase modulation wave form.

that of curve 1 using the old wave form. The secondary curve, which has the same sensitivity as curve 4 using the old wave form, has a concentration SNR which is better by approximately the expected factor of 1.7 (equal to $(12/4)^{1/2}$). This indicates that the two curves in Figure 10B can satisfactorily cover the range from 0.1 to 10 000 µg/mL.

Figure 11 contains concentration error plots for magnesium (285.21 nm) using the bi-Gaussian (Figure 11A) and the staircase (Figure 11B) modulation wave forms. Figure 11A suggests that curves 1–4 are useful and provide relative concentration errors of 0.01 or less. Figure 11B indicates that the same concentration range (0.01 to 10 000 µg/mL) can be covered satisfactorily with only 2 curves. Although the secondary curve does not provide RCE values which are quite as low as those obtained by using curves 2 and 3 with the old wave form at their minimum RCE values, relative concentration precision over the entire range was better than 0.008.

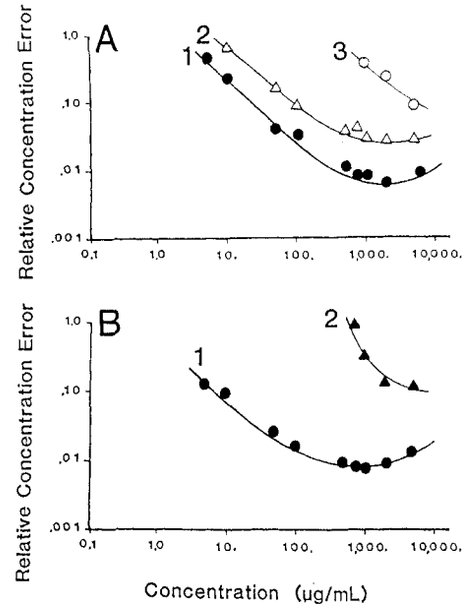

Figure 12. Relative concentration error curves for iron (248.327 nm) in an air–acetylene flame using: (A) bi-Gaussian and (B) staircase modulation wave form.

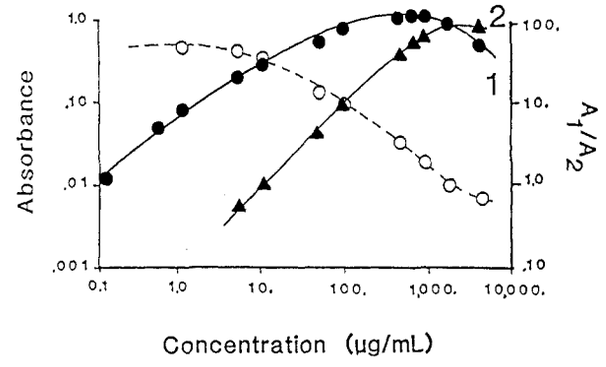

Figure 13. Calibration curves for magnesium (285.213 nm) (—) and the ratio of the absorbance of the two curves (--) as a function of concentration.

The solution concentration above which the secondary curve exhibits a lower concentration error depends upon the absorption sensitivity of the chosen analytical line. Thus for magnesium (Figure 11B), the crossover between the two curves occurs at about 100 µg/mL, whereas for the less sensitive copper (Figure 10B), the crossover does not occur until about 1000 µg/mL. We can therefore expect that for even less sensitive elements, the crossover may occur above the concentration range of interest. Iron (248.327 nm) is an example. Figure 12 contains concentration error plots for this line using the bi-Gaussian (Figure 12A) and the staircase (Figure 12B) modulation wave forms. Both of these plots show that the only useful curve up to 5000 µg/mL is curve 1 for both modulation wave forms. The primary curve using the staircase wave form has somewhat improved RCE values. As mentioned before, this is due to the improved sensitivity of this analytical calibration curve. This verifies that multiple curves are not useful for every element.

Calibration Curve Reversal. Although multiple calibration curves provide an extended dynamic concentration range, calibration curve reversal is still a problem for some of the elements of interest. Figure 13 illustrates this with a plot of both the primary and secondary calibration curves for magnesium (285.21 nm). In addition, this figure contains a plot of the ratio of A_1/A_2 (A_1 and A_2 are the absorbance values for curves 1 and 2, respectively) as a function of concentration. This plot illustrates the usefulness of the A_1/A_2 ratio in de-

Table I. Standard Reference Materials Results

std ref material	element	certified value	SIMAAC value[a]	AAL value[b]
Wheat Flour, No. 1567	Mn	8.5 ± 0.5 μg/g	9.7 ± 0.4	7.9 ± 0.2
	Zn	10.6 ± 1.0 μg/g	12.6 ± 1.3	9.9 ± 0.5
	Fe	18.3 ± 1.0 μg/g	14.8 ± 1.2	16.2 ± 0.5
	Cu	2.0 ± 1.0 μg/g	2.0 ± 0.2	2.0 ± 0.6
	Mg		378 ± 8 μg/g	373 ± 11
	K	0.136 ± 0.004%	0.124 ± 0.003	0.126 ± 0.003
Rice Flour, No. 1568	Mn	20.1 ± 0.4 μg/g	22.4 ± 0.9	19.5 ± 1.0
	Zn	19.4 ± 1.0 μg/g	19.9 ± 1.4	18.7 ± 4.6
	Fe	8.7 ± 0.6 μg/g	5.6 ± 0.9	7.0 ± 0.3
	Cu	2.2 ± 0.3 μg/g	2.4 ± 0.1	2.2 ± 0.2
	K	0.112 ± 0.002%	0.108 ± 0.002	0.110 ± 0.003
Bovine Liver, No. 1577	Mn	10.3 ± 1.0 μg/g	10.8 ± 0.2	10.1 ± 0.6
	Fe	268 ± 8 μg/g	264 ± 4	254 ± 7
	Ce	193 ± 10 μg/g	187 ± 2	197 ± 11
	Mg	604 ± 9 μg/g	555 ± 12	594 ± 13
	Na	0.243 ± 0.013%	0.249 ± 0.026	0.257 ± 0.087
	K	0.97 ± 0.06%	1.00 ± 0.01	0.92 ± 0.01
Spinach, No. 1570	Mn	165 ± 6 μg/g	158 ± 13	165 ± 8
	Zn	50 ± 2 μg/g	55 ± 2	47 ± 2
	Fe	550 ± 20 μg/g	556 ± 15	558 ± 12
	Cu	12 ± 2 μg/g	12 ± 1	12 ± 1
	Mg		0.920 ± 0.030	0.870 ± 0.050
	K	3.56 ± 0.03%	3.29 ± 0.09	3.57 ± 0.29

[a] $n = 3$. [b] $n = 8$ for all reference materials but spinach (no. 1570) where $n = 3$.

termining whether or not a given absorbance value falls on the reverse side of the calibration curve. This means that absorbances of unknowns which would normally provide nonunique solutions for concentration now can be determined successfully. As an example, calibration standards of 100 μg/mL and 2000 μg/mL have nearly identical absorbance values on the primary curve (~0.74 absorbance units) but their A_1/A_2 values differ by almost an order of magnitude. A simple algorithm was developed to compare sample A_1/A_2 and A_1/A_2 ratios of the calibration standards to determine if the sample falls on the reverse side of either or both calibration curves. This ratio diagnostic could also be used to allow the analyst to compute valid concentrations on the reverse side of the calibration curves by comparing the sample A_1/A_2 ratio to the A_1/A_2 ratios of the standards which bracket the sample absorbance value.

Accuracy. The final criterion by which every analytical method must be evaluated is accuracy. For this reason, it was essential to ensure that accuracies were acceptable when using the new two curve method. With the new method, concentration values from the two curves were again weighted by the square of their concentration SNR's to compute a final weighted concentration. Presented here are results obtained for the four National Bureau of Standards (NBS) standard reference materials (SRM's).

Table I summarizes the results of the analyses. Results are reported on a dry weight (μg/g or %) basis. SIMAAC results using the new wave form are compared to NBS certified values as well as single element line source atomic absorption (AAL) values. AAL values were obtained by using different subsamples but identical sample preparation procedures. AAL analyses were performed on an optimized single element basis and samples were diluted so that measurements could be made in the linear range of the calibration curve for each element. Simultaneous multielement analyses using the SIMAAC system were performed on the original sample digests. No additional dilutions were necessary because of the extended dynamic concentration range the system provides. Compromise atomization conditions were employed (*4*).

SIMAAC accuracies ranged from 91 to 110% while AAL accuracies ranged from 93 to 106%. Iron values were low for both of the flour SRM's for both SIMAAC and AAL analyses. Subsequent studies verified that the digestion procedure used does not provide complete solubilization of the iron. Alternate digestion procedures are currently being studied (*6*). SIMAAC results provided average accuracies of ±6% compared to ±4% for AAL analyses. Average accuracies of ±6% for SIMAAC analyses are satisfactory considering that only a single dilution is required for simultaneous multielement analyses. In addition, these data suggest that compromise conditions have only a slight adverse effect on the accuracy of the analysis of these elements. With regard to precision, SIMAAC results generally have relative standard deviations (RSD's) of less than 8%. The notable exceptions are zinc results which have larger RSD's due to the poor signal-to-noise ratio for zinc which is the result of the poor UV intensity of the continuum source. RSD's for bovine liver results were less than 2.0% for every element. This is most likely due to the fact that elemental concentrations are higher in this reference material than in the others analyzed. The average RSD for all SIMAAC analyses was 5% while the average RSD for AAL analyses was 8%. This is perhaps somewhat surprising considering that, on the average, SIMAAC detection limits are 2- to 3-fold poorer than line source detection limits (*1*, *2*). The poorer precision of the AAL data in this work may reflect the fact that the samples were diluted into the linear range for each element, which is generally below the concentration corresponding to the minimum concentration error (compare Figures 9 and 11).

CONCLUSIONS

This work clearly shows that the staircase modulation wave form is an improvement over the bi-Gaussian modulation wave form. The new two curve method provides an extended dynamic concentration range, faster and easier absorbance computations, an improved SNR on the less sensitive curve, the ability to test for calibration curve reversal, and acceptable accuracies and precisions for multielement analyses. Additionally, the two curve method has a significant time advantage with regard to the final calibration and curve fitting program. A detailed printout with blank subtracted data and individual curve fitting results for each element as well as a final report summary took only 25 min to run for 10 standards and 13 samples for 9 elements using the new two curve method. With

the old six curve method this would have required approximately 60 min.

ACKNOWLEDGMENT

The authors thank F. E. Greene for her assistance with the line source analyses of the standard reference materials.

Registry No. Mn, 7439-96-5; Zn, 7440-66-6; Fe, 7439-89-6; Cu, 7440-50-8; Mg, 7439-95-4.

LITERATURE CITED

(1) Harnly, J. M.; O'Haver, T. C. *Anal. Chem.* **1981**, *53*, 1291-1298.
(2) Harnly, J. M.; O'Haver, T. C.; Golden, B.; Wolf, W. R. *Anal. Chem.* **1979**, *51*, 2007-2014.
(3) Harnly, J. M.; Miller-Ihli, N. J.; O'Haver, T. C. *J. Autom. Chem.* **1982**, *4*, 54-60.
(4) Harnly, J. M.; Kane, J. S.; Miller-Ihli, N. J. *Appl. Spectrosc.* **1982**, *36*, 637-643.
(5) Wolf, W. R. In "Human Nutrition Research, Beltsville Symposia In Agricultural Research"; Allanheld, Osmun and Co.: Totowa, NJ, 1981; Volume 4, pp 175-196.
(6) Kuennen, R. W.; Wolnik, K. A.; Fricke, F. L.; Caruso, J. A. *Anal. Chem.* **1982**, *54*, 2146-2150.

RECEIVED for review June 30, 1983. Accepted October 20, 1983. Presented in part at the 1982 Federation of Analytical Chemistry and Spectroscopy Societies Meeting (Paper No. 301), Philadelphia, PA.

Molecular Photoluminescence Spectrometry with Hydride Generation for Determination of Trace Amounts of Antimony and Arsenic

Hiroaki Tao,* Akira Miyazaki, Kenji Bansho, and Yoshimi Umezaki[1]

National Research Institute for Pollution and Resources, Yatabe, Ibaraki 305, Japan

Molecular photoluminescence detection was developed for the determination of antimony and arsenic. Antimony and arsenic were generated as hydrides and irradiated with ultraviolet light. The broad continuous emission bands were observed in the ranges about 240–750 nm and 220–720 nm, and the detection limits were 0.6 ng and 9.0 ng for Sb and As, respectively. Some characteristics of photoluminescence phenomenon were made clear from spectroscopic observations. After the interference study, the method was successfully applied to the determination of antimony in river water and seawater.

The hydride generation technique has become widely used in spectrometric analysis. It allows the separation and preconcentration of an analyte from the sample matrix, thereby providing an improved detection limit and relative freedom from detector interference. For the final measurement, atomic spectrometries, e.g., atomic absorption (*1*), emission (*2–4*), and fluorescence (*5*) spectrometry, have been mainly used, although molecular emission spectrometry (*6*, *7*), mass spectrometry (*8*), and thermal conductivity detectors (*9*) have also been employed. In addition, chemiluminescence spectrometry with ozone oxidation of hydrides has been proposed recently (*10*, *11*).

Molecular photoluminescence spectrometry has good sensitivity and selectivity for some organic or inorganic materials and has been applied to the biochemical and environmental spheres as fluorescence spectrometry (*12*). However, to our knowledge, it has not been applied so far to the determination of hydrides. In the present paper, molecular photoluminescence detection of some hydrides is investigated. Intense luminescence spectra are observed in the region 240–750 nm and 220–720 nm when stibine and arsine are exposed to ultraviolet light of wavelength 200–240 nm, respectively. The aim of this work is to demonstrate that molecular photoluminescence spectrometry is a very sensitive and selective method for the determination of some hydrides. In the case of stibine, the molecular species which luminesces is also discussed and an interference study is carried out. The method has been successfully applied to the determination of antimony in river water and seawater. Although the present report is concerned only with antimony determination, the interference study shows that other hydrides, especially arsenic, can be determined in a similar way. Since this method does not need a flame, it is suitable for an automated system and will provide simple sequential multielement analysis capability of nanogram amounts of some hydrides by coupling to gas chromatography.

EXPERIMENTAL SECTION

Apparatus. The hydride generation system with a liquid nitrogen trap is shown in Figure 1. The hydride generated in the reaction vessel was swept into the liquid N_2 U-trap (25 cm × 3.3 mm i.d., fully packed with 24–35 mesh glass beads). A U-tube with Drierite (25 cm × 1 cm i.d., 8 mesh) was used to remove the water vapor from the reaction solution. The hydride frozen in the liquid N_2 trap was then released, by inserting the trap in hot water, and was introduced into the cell with a helium flow of 1 mL/min by a peristaltic pump (Technicon, Model II). The hydride was then irradiated with light of 210 nm, and the resulting luminescence intensity at 325 nm was monitored with a fluorescence spectrometer. The luminescence detection was made by a Hitachi Model, 650-60 fluorescence spectrometer with a 150-W xenon lamp (Ushio, type UXL-157) and R-928F photomultiplier (Hamamatsu Photonics). The maximum slit width (spectral band-pass 20 nm) was used unless otherwise stated. The cell was a conventional fluorescence cell and the volume (4.4 mL) was reduced to 1.4 mL with a brass spacer to avoid the large dead volume.

Chemicals. A stock solution of Sb (1000 μg/mL) was prepared by dissolving $SbCl_3$ in 3 M HCl solution. A stock solution of As (1000 μg/mL) was prepared by dissolving As_2O_3 in a minimum amount of 0.2 M NaOH and diluting the solution with a small amount of concentrated H_2SO_4 to the final H_2SO_4 concentration of 0.01 M. Stock solutions of Sn and Te (1000 μg/mL) were prepared by dissolving $SnCl_2 \cdot 2H_2O$ and Na_2TeO_3 in diluted HCl solutions. Stock solutions of Ge and Se (1000 μg/mL) were prepared by dissolving K_4GeO_4 and SeO_2 in diluted KOH solution

[1] Present address: Government Industrial Research Institute, Chugoku, Hiro-machi, Kure-shi, Hiroshima 737-01, Japan.

0003-2700/84/0356-0181$01.50/0